
Visual Instruction Tuning with Chain of Region-of-Interest

Yixin Chen*

Amazon Web Services

Shuai Zhang

Amazon Web Services

Boran Han

Amazon Web Services

Bernie Wang

Amazon Web Services

Abstract

High-resolution (HR) images are pivotal for enhancing the recognition and understanding capabilities of multimodal large language models (MLLMs). However, directly increasing image resolution can significantly escalate computational demands. In this study, we propose a method called Chain of Region-of-Interest (**CoRoI**) for Visual Instruction Tuning, aimed at alleviating the computational burden associated with high-resolution images for MLLMs. Drawing inspiration from the selective nature of the human visual system, we recognize that not all regions within high-resolution images carry equal importance. CoRoI seeks to identify and prioritize the most informative regions, thereby enhancing multimodal visual comprehension and recognition while circumventing the need for processing lengthy HR image tokens. Through extensive experiments on 11 benchmarks, we validate the efficacy of CoRoI across varying sizes, ranging from 7B to 34B in parameters. Our models consistently demonstrate superior performance across diverse multimodal benchmarks and tasks. Notably, our method outperforms LLaVA-NeXT on almost all benchmarks and our finetuned 34B model surpasses proprietary methods like Gemini Pro 1.0 on six benchmarks, as well as outperforming GPT-4V on MMB, SEED-I, and MME.

1 Introduction

Multimodal Large Language Models (MLLMs) [56, 1, 37, 65, 60, 35, 66, 59, 6] have demonstrated outstanding performance across a variety of multimodal tasks. Despite this, their recognition and comprehension capabilities are limited by low-resolution image inputs, as these models are generally trained with fixed resolutions such as 336×336 or 448×448 [35, 37, 15]. This inflexible design makes it challenging for them to identify small and blurry objects, capture crucial details, and generate fine-grained results.

Recent approaches have started incorporating high-resolution images to enhance MLLMs' performance [42, 22, 61, 36, 57, 33]. For instance, LLaVA-Next [36] extends LLaVA-1.5 [35] by integrating high-resolution image tokens to grasp more visual details. InternLM-XComposer2-4KHD [18] uses compression techniques to accommodate more tokens for higher-resolution images. Additionally, LLaVA-HR [43] utilizes mixture-of-resolution adapters to fuse low- and high-resolution. Other methods [22, 61] employ cross-attention layers to integrate high-resolution and low-resolution image tokens to avoid directly encoding high-resolution image tokens in LLM backbones. All these methods underscore the importance of high-resolution images in MLLMs.

*Work done at Amazon

However, existing solutions have several disadvantages, which we summarize as follows: (1) Increasing resolution in a brute-force manner leads to a significant increase in token lengths (e.g., 5,329 tokens for a $1,022 \times 1,022$ resolution image [35]), consequently resulting in quadratic growth in operations and computational demands for LLMs; (2) Commonly used vision encoders, such as pretrained ViTs [19], are typically trained on low-resolution images (e.g., 224×224), which can cause performance degradation when processing high-resolution images; (3) High-resolution image tokens cover all spatial locations indiscriminately, lacking focus on the areas relevant to the given queries. This can result in unnecessary computational overhead by processing regions that are irrelevant to the given questions; (4) Methods such as those in [22, 61] can reduce the input tokens for LLMs, but they still require the cross-attention to be conducted between all high-resolution tokens and the low-resolution tokens. This may potentially result in many irrelevant or meaningless connections between tokens.

To address these issues, we propose a method named Chain of Region-of-Interest (**CoRoI**) for visual instruction fine-tuning. CoRoI consists of two main steps: (1) *Chain of Region-of-Interest Extraction*: CoRoI captures the most informative regions from high-resolution images by integrating visual clues (i.e., low-resolution (LR) image tokens) and language clues (i.e., text questions). Mimicking human eye movement, we design a region-of-interest movement mechanism that can generate a sequence of visually relevant regions from high-resolution images. This approach eliminates the need to process the entire high-resolution image, thereby reducing computational demands; (2) *Incorporating Chain of RoI into LLMs*: CoRoI injects the extracted regions of interest into the hidden layers of the LLMs, enabling cross-attention with the corresponding low-resolution image tokens. This ensures a tight interaction between the high-resolution and low-resolution image tokens at different abstraction levels. To summarize, our contributions are:

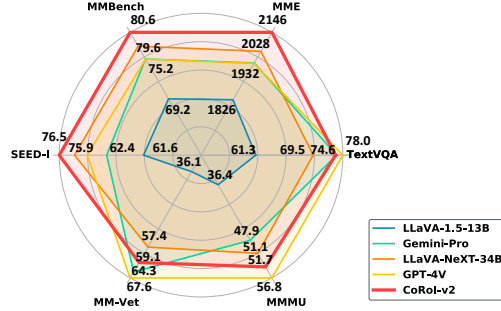


Figure 1: Zero-shot performance comparison with LLaVA-1.5, LLaVA-NeXT, Gemini-Pro 1.0, and GPT-4V.

- We proposed CoRoI, a visual instruction fine-tuning method by enforcing the model to only focus on relevant regions of high-resolution images, allowing the model to handle high-resolution images effectively and efficiently.
- We applied CoRoI to open-source LLMs with parameter sizes ranging from 7B to 34B and built three model variants, demonstrating that CoRoI can consistently enhance multimodal recognition and comprehension capabilities.
- We conducted experiments on 11 benchmark datasets, including SEED-Image [32], MMBench [38], MME [20], MM-Vet [63], MMMU [64], MathVista [40], TextVQA [54], GQA [23], VQA v2 [7], VizWiz [21], and ScienceQA-Image [41]. Our results show that CoRoI achieves state-of-the-art performance compared to open-source and proprietary models, consistently outperforming LLaVA-NeXT [36] and Gemini Pro 1.0 [56], occasionally matching or surpassing proprietary models like GPT-4V [1].
- We conducted comprehensive model analyses, including ablation and case studies, to elucidate the inner workings and demonstrate the model’s performance in real-world scenarios.

2 Related Work

Multimodal Large Language Models The recent advancements in LLMs (e.g., ChatGPT [10], GPT-4 [48], LLaMA [58], Claude [3], and Mixtral [27]) have sparked a growing interest in scaling up multimodal large language models (MLLMs). By integrating LLMs with vision encoders like ViT [19] and CLIP [49], these models can handle various visual-language understanding tasks such as visual question answering and image captioning [65, 34, 37, 35]. MLLMs mainly differ in their methods of combining LLMs with visual encoders. For example, some methods inject image tokens into the hidden layers of LLMs [65, 6, 8], while others project them into the text token embedding space and treat them equally as text tokens [37, 35]. Additionally, it is possible

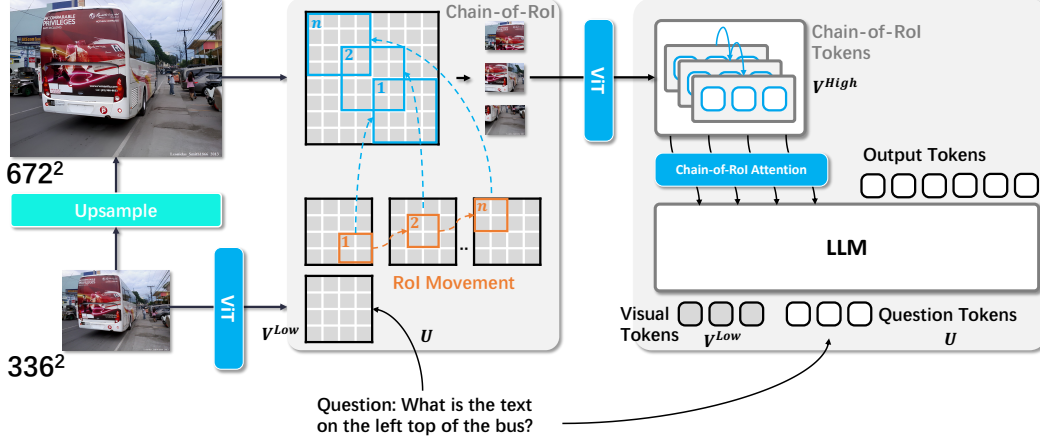


Figure 2: Illustration of CoRoI. Low-resolution images and text clues are used to identify a chain of regions of interest in the corresponding high-resolution images. These regions are then injected into the hidden states of the LLMs to facilitate answer generation. Here, $m = 1$, $\lambda = 2$, $n = 3$.

to train MLLMs from scratch without using existing LLMs as backbones. These methods typically tokenize data from different modalities into the same embedding space and use them in an interleaved manner [60, 25, 24, 52, 67, 39, 55] with causal language modeling training objectives.

MLLMs with High-Resolution Images Existing MLLMs are typically trained with fixed resolutions, such as 336×336 and 448×448 [37, 35, 65, 60, 66, 14, 59, 6]. This limitation makes it challenging for these models to perceive small or blurry objects in images, leading to failures in tasks such as OCR and document understanding, where high resolution is necessary to make details clear and recognizable and allow for finer distinctions between objects. Recently, many methods have introduced high-resolution inputs to enhance MLLMs’ capability by providing more fine-grained visual features [42, 22, 61, 36, 57, 33]. Examples include LLaVA-Next [36], LLaVA-HR [43], OtterHD [33], InternLM-XComposer2-4KHD [18] and InternVL 1.5 [15]. Processing high-resolution images is a nontrivial task, particularly because most commonly used vision encoders (e.g., ViT) cannot handle high-resolution images directly. To avoid information loss, many methods [35, 36, 22] divide high-resolution images into smaller patches and encode them independently. These patches are then concatenated for further processing. While this approach can enhance performance, it also results in a quadratic increase in computational cost due to the long context length when working with LLMs. Differing from existing methods, CoRoI can easily handle high-resolution images via the proposed chain of region-of-interest mechanism. This method extracts regions of interest from high-resolution images leveraging both language and visual signals. These identified regions of interest are then used to facilitate LLM generation. By focusing solely on the most informative regions, it circumvents the necessity to encode the entire high-resolution image. Moreover, the entire process is differentiable and does not require human intervention.

3 Method

Figure 2 illustrates the proposed framework. It operates by first upsampling the resolution of input low-resolution images to yield multiple high-resolution images with m different scaling factors $\lambda \in \{2, 3, 4, \dots\}$. Subsequently, the low-resolution image and text questions are employed to pinpoint the most informative and relevant regions via the chain of region-of-interest extraction module. Once identified, corresponding regions are extracted from the high-resolution image as clips. These clips, with high-quality local information, are then injected into the hidden layers of the LLM to enhance the generation accuracy.

Before delving into the model details, let us examine two real-world examples in Figure 3, using the model trained via CoRoI. Remarkably, CoRoI empowers the model to capture the most informative and relevant regions from the given high-resolution images, tailored to the asked questions.



Figure 3: CoRoI enables the model to extract a chain of region-of-interest during inference. We used variant: CoRoI-v2 (Hermes-2-Yi-34B). The selected regions are closely relevant to the asked questions. We also provide the answers given by GPT-4V.

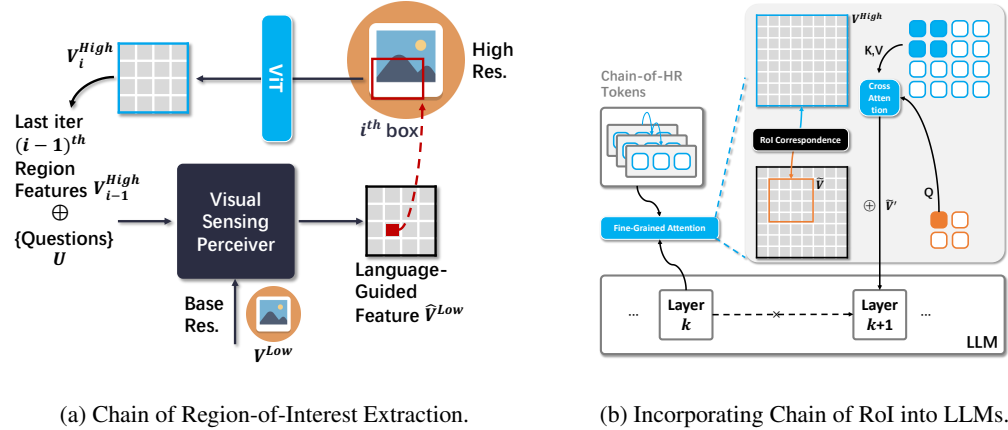


Figure 4: Modules design details.

3.1 Chain of Region-of-Interest Extraction

Here, we introduce the chain of region-of-interest extraction methodology (shown in Figure 4(a)).

Region-of-Interest Selection To select the first high-resolution region, first, a cross-attention block is employed to process the low-resolution image feature, $\mathbf{V}^{Low} \in \mathbb{R}^{h \times w \times d}$ (extracted via ViT). This feature undergoes a self-attention layer to capture inherent visual relationships, followed by a cross-attention layer interacting with the question token embeddings \mathbf{U} . This integration enables the model to incorporate language clues. The results are then fed into a feed-forward layer, resulting in an output denoted as $\hat{\mathbf{V}}^{Low} := f_{\theta_v}(\mathbf{V}^{Low}) \in \mathbb{R}^{h \times w \times 1}$. Next, to extract the most informative region, we employ a sliding window approach to traverse $\hat{\mathbf{V}}^{Low}$ and obtain a couple of candidate regions. The region with the highest pooled (average pooling) value is considered the current most informative region. Once we obtain the region location, we can extract the corresponding image clip from the high-resolution images. The sliding window is designed as follows: if the low-resolution image has dimensions of 336×336 and $\hat{\mathbf{V}}^{Low}$ is of size 24×24 , and the high-resolution image has dimensions of $\lambda 336 \times \lambda 336$, the sliding window size would be $\lceil 24/\lambda \rceil \times \lceil 24/\lambda \rceil$. We set the stride size to 1 and the padding size to 0 by default. The extracted region clip from HR images will be dimension of 336×336 .

Region-of-Interest Movement Inspired by how humans capture information with their eyes—*focusing on one region of interest and then moving to the next for further clues*—we devised a region-of-interest movement mechanism. This mechanism operates iteratively, producing a sequence/chain of regions of interest. Initially, only the text question is used as the key/value for the RoI selection process (see paragraph above). After identifying the first region of interest from HR images, we encode this region clip using ViT to obtain a feature tensor \mathbf{V}_i^{High} , where $i = 0, \dots, n$, represents the i -th iteration. We then concatenate \mathbf{V}_i^{High} with the question token \mathbf{U} and use the concatenated tensor as the key&value for the *cross-attention layer* mentioned above, allowing us to identify the second region of interest. As the process goes on, we will obtain n regions of interest, forming a chain of regions of interest. If we have m high-resolution images of different scaling factors, we will get mn regions of interest in the end.

3.2 Incorporating Chain of RoI into LLMs

We integrate the extracted chain of regions of interest into LLMs (shown in Figure 4(b)). Given that the number of regions, mn , can be large, we opt not to use them directly as input tokens for the LLM. Instead, we inject them into the LLM’s hidden layers using a cross-attention module.

Cross Attention between RoI and LR Tokens In our framework, low-resolution tokens are directly used as the input for LLMs. To inject the i^{th} region of interest into the k^{th} layer of the LLM, we first identify the positions of the corresponding low-resolution tokens and extract the hidden states $\tilde{\mathbf{V}}_{i,k}^{Low}$ at layer k . Next, we perform cross-attention between the region of interest feature \mathbf{V}_i^{High} and $\tilde{\mathbf{V}}_{i,k}^{Low}$. The cross-attention module consists of a single linear layer and a layer normalization for the query, key, and value, respectively. Here, $\tilde{\mathbf{V}}_{i,k}^{Low}$ serves as the query, while \mathbf{V}_i^{High} acts as the key and value.

Inject RoI into LLMs as Residual The output, defined as $f_{\theta'}(\tilde{\mathbf{V}}_{i,k}^{Low}, \mathbf{V}_i^{High})$, where θ' is the parameters of cross-attention layer, is then used as a residual and added back to $\tilde{\mathbf{V}}_{i,k}^{Low}$. As such, the hidden state is modified to $\tilde{\mathbf{V}}_{i,k}^{Low} + f_{\theta'}(\tilde{\mathbf{V}}_{i,k}^{Low}, \mathbf{V}_i^{High})$. This process injects high-resolution features into the LLMs with minimal additional cost. Layer normalization between LLM layers helps mitigate instability caused by the added residual.

3.3 Model Training

We have two training stages, with the vision encoder remaining frozen throughout.

1st stage - Projector Pretraining: In this stage, we perform modality alignment between ViT and LLM using a trainable projector, following the approach in [37], without incorporating the proposed modules. All other components except for the projector are frozen in this stage.

2nd stage - Visual Instruction Fine-Tuning: Here, we employ our modules and activate all parameters except the vision encoder. The model is trained by minimizing the causal language modeling loss: $\ell = -\sum_{i=1}^{|y|} \log p_{\theta}(y_i | \hat{y}_{1:i-1}, q)$, where $\theta \leftarrow (\theta^{\text{LLM}}, \theta^v, \theta')$ represents the model’s trainable parameters (θ^{LLM} being the LLM’s parameters), y_i is the ground-truth target, and $\hat{y}_{1:i-1}$ denotes the $i-1$ preceding tokens of the output y_i .

4 Experiment

4.1 Experimental Setup

Implementation Details We resized all raw training images to 336×336 pixels, treating this as the low/base resolution. We then used bilinear interpolation to generate the corresponding high-resolution images. By setting $m = 3$ and λ to 2, 3, and 4, the resulting high-resolution images have dimensions of 672×672 , 1008×1008 , and 1344×1344 pixels, respectively. The number of RoI (n) in each chain is set to 4. We employed a CLIP-pretrained ViT-L [49] model as the vision encoder, which remained frozen throughout the training process. All the training processes were conducted for one epoch using the AdamW optimizer and a cosine learning rate schedule, without further tuning. The initial learning rate was set to 1×10^{-3} for projector pretraining and 2×10^{-5} for visual instruction

Table 1: Comparison with state-of-the-art methods on comprehensive zero-shot benchmarks. Res.* means the visual resolution of LLM image input tokens.

Method	LLM	Res.*	SEED ^I	MMB	MME	MM-Vet	MMMU _v	MathVista
MobileVLM-V2 [16]	Vicuna-7B	336 ²	–	69.2	1560	–	–	–
InstructBLIP [17]	Vicuna-7B	224 ²	58.8	36.0	–	26.2	–	25.3
InstructBLIP [17]	Vicuna-13B	224 ²	–	–	1213	25.6	–	–
Qwen-VL [9]	Qwen-7B	448 ²	62.3	38.2	–	–	–	–
Qwen-VL-Chat [9]	Qwen-7B	448 ²	65.4	60.6	1488	–	35.9	–
Shikra [12]	Vicuna-13B	224 ²	–	58.8	–	–	–	–
IDEFICS-80B [31]	LLaMA-65B	224 ²	53.2	54.5	–	–	–	–
LLaVA-1.5 [35]	Vicuna-7B	336 ²	–	65.2	1511	31.1	–	–
LLaVA-1.5 [35]	Vicuna-13B	336 ²	68.2	69.2	1531/295	36.1	36.4	27.6
CoRoI-v1	Mistral-7B	336 ²	72.0	69.0	1528/328	44.5	36.8	36.2
OtterHD [33]	Fuyu-8B	1024 ²	–	53.6	1314	–	–	–
CogVLM-Chat [61]	Vicuna-7B	490 ²	72.5	63.7	–	51.1	41.1	34.5
LLaVA-HR-X [43]	Vicuna-13B	1024 ²	–	–	1487	35.5	–	–
LLaVA-NeXT [36]	Vicuna-7B	672 ²	70.2	68.1	1519/332	43.9	35.8	34.6
LLaVA-NeXT [36]	Vicuna-13B	672 ²	71.9	70.7	1575/326	48.4	36.2	35.3
LLaVA-NeXT [36]	Hermes-2-Yi-34B	672 ²	<u>75.9</u>	<u>79.6</u>	1631/397	57.4	51.1	46.5
CoRoI-v2	Mistral-7B	672 ²	73.1	69.9	1540/339	49.6	36.9	37.5
CoRoI-v2	Hermes-2-Yi-34B	672 ²	76.5	80.6	1662/484	59.1	<u>51.7</u>	<u>47.2</u>
Gemini Pro 1.0 [56]	Private	–	62.4	75.2	1496/436	64.3	47.9	45.2
Qwen-VL-Plus [9]	Private	–	72.7	66.2	1681/502	–	45.2	43.3
GPT-4V [1]	Private	–	69.1	75.1	1409/517	67.6	56.8	49.9


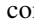
Table 2: Comparison with state-of-the-art methods on Vision-Language tasks. Res.* means the visual resolution of LLM image input tokens.


































Method	LLM	Res.*	TextVQA (VQA ^T)	GQA	VQAv2	Vizwiz	SQA ^I
MobileVLM-V2[16]	Vicuna 7B	336 ²	62.3	62.6	–	–	74.8
InstructBLIP [17]	Vicuna-7B	224 ²	50.1	49.2	–	34.5	60.5
InstructBLIP [17]	Vicuna-13B	224 ²	50.7	49.5	–	33.4	63.1
Qwen-VL [9]	Qwen-7B	448 ²	63.8	59.3	78.8	35.2	67.1
Qwen-VL-Chat [9]	Qwen-7B	448 ²	61.5	57.5	78.2	38.9	68.2
Shikra [12]	Vicuna-13B	224 ²	–	–	77.4	–	–
IDEFICS-80B [31]	LLaMA-65B	224 ²	30.9	45.2	60.0	36.0	–
LLaVA-1.5 [35]	Vicuna-7B	336 ²	58.2	62.0	78.5	50.0	66.8
LLaVA-1.5 [35]	Vicuna-13B	336 ²	61.3	63.3	80.0	53.6	71.6
CoRoI-v1	Mistral-7B	336 ²	64.8	64.5	81.2	56.7	73.1
CogVLM-Chat [61]	Vicuna-7B	490 ²	70.4	–	82.3	–	–
LLaVA-HR-X [43]	Vicuna-13B	1024 ²	<u>70.9</u>	65.2	82.6	56.6	68.0
LLaVA-NeXT [36]	Vicuna-7B	672 ²	64.9	64.2	81.8	57.6	70.1
LLaVA-NeXT [36]	Vicuna-13B	672 ²	67.1	65.4	82.8	60.5	73.6
LLaVA-NeXT [36]	Hermes-2-Yi-34B	672 ²	69.5	<u>67.1</u>	<u>83.7</u>	63.8	<u>81.8</u>
CoRoI-v2	Mistral-7B	672 ²	69.7	65.1	82.7	59.6	73.4
CoRoI-v2	Hermes-2-Yi-34B	672 ²	74.0	67.8	84.0	<u>63.2</u>	82.8

fine-tuning for all models, except for Hermes-2-Yi-34B [5], where the instruction fine-tuning learning rate was set to 1×10^{-5} . All experiments were performed on 8 H100 GPUs with an accumulative batch size of 128, initialized using the DeepSpeed Zero3 [50] configuration.

Model Variants We used Mistral-7B [26] and Hermes-2-Yi-34B [5] as the LLM backbones. For each backbone, we created two model versions by varying the input tokens. In the first version (denoted as CoRoI-v1), we used 336×336 images, corresponding to 576 tokens as the LLM’s input. In the second version (denoted as CoRoI-v2), we also used 672×672 images as input for the LLMs, resulting in a total of 2880 tokens (576 tokens from the 336×336 images plus 2304 tokens from the 672×672 images). In this case, the RoI features were only injected into the tokens from the 336×336 images. All in all, the LLM backbone does not have to deal with a very long context length.

Datasets For model optimization, we create high-quality data to enhance cross-modality understanding and generation. This dataset includes LLaVA-558K and ALLaVA-Caption-4V [11] (~ 1.2 million caption pairs) for modality alignment during projector pretraining and LLaVA-

Table 3: Ablation on model design. In upper part,  is the improvement against LLaVA-1.5, and in lower part  indicates performance degradation compared with CoRoI-v1.

Method	Res.	HR Res.	LLM Tokens	TextVQA (VQA ^T)	MMBench	MME
LLaVA-1.5	336 ²	—	576	58.2	65.2	1510
Apply CoRoI:						
CoRoI-v1	336 ²	2/3/4×	576	63.3 	69.0 	1524 
w/o Visual Movement	336 ²	2/3/4×	576	62.5 	68.4 	1513 
Layers Location (k):						
+ {15} th layer	336 ²	2/3/4×	576	62.6 	68.0 	1423 
+ {7, 15, 23} th layer	336 ²	2/3/4×	576	63.0 	68.4 	1431 
RoI Nums (n):						
+ 1 RoIs	336 ²	2/3/4×	576	62.4 	68.5 	1421 
+ 2 RoIs	336 ²	2/3/4×	576	61.9 	68.7 	1434 
Multi-scale HR Resolution (m, λ):						
+ 2×	336 ²	2×	576	61.5 	67.4 	1486 
+ 3×	336 ²	3×	576	62.2 	68.3 	1454 
+ 4×	336 ²	4×	576	62.7 	68.1 	1473 
+ 2/3×	336 ²	2/3×	576	62.1 	68.5 	1487 
+ 3/4×	336 ²	3/4×	576	62.0 	68.6 	1496 

665K (made up of LLaVA-Instruct-158K [37], ShareGPT-40K [2], VQAv2 [7], GQA [23], OKVQA [44], OCRVQA [47], A-OKVQA [51], RefCOCO [62] and VG [30]) without TextCaps [53], ShareGPT4V [13], LAION-GPT4V [4], DocVQA [46], AI2D [29], ChartQA [45], DVQA [28] and ALLaVA-Instruct-4V [11] (~1.5 million single- or multi-round conversations) for visual instruction fine-tuning. We evaluated our models on widely-adopted zero-shot multimodal benchmarks, including SEED [32] (Image), MMB [38] (MMBench), MME [20], MM-Vet [63], MMMU [64], and MathVista [40] datasets. Additionally, we reported results on well-known visual question answering datasets, such as VQA^T (TextVQA), GQA [23], VQA v2 [7], VizWiz [21], and SQA^I [41] (ScienceQA-Image).

4.2 Model Quantitative Analysis

4.2.1 Multimodal Instruction-Following

Comprehensive Multimodal Benchmarks In Table 1, we compare our approach with previous leading open-source and closed-source methods across various comprehensive zero-shot multimodal benchmarks. These benchmarks assess the model’s visual understanding, reasoning, multidisciplinary abilities, and even logical thinking and math capabilities. Overall, we observe a consistent performance boost from the three variants over open-source models with the same parameter size and input resolutions, confirming the effectiveness of our proposed method. Our most performant variant, CoRoI-v2 (Hermes-2-Yi-34B), surpasses proprietary closed-source models such as Gemini Pro 1.0 [56] on 5/6 benchmarks, and outperforms Qwen-VL-Plus [9] in most cases. It also occasionally performs better than or is on par with GPT-4V [1] on all the benchmarks.

Visual Question Answering Benchmarks In Table 2, we also present a comparison of CoRoI with existing methods on widely used visual question answering benchmarks. Datasets such as TextVQA (VQA^T) require the model to have certain OCR (Optical Character Recognition) capabilities to read and reason over the text and scene in the given images. Similarly, noticeable performance improvements can be observed on the five datasets compared to baselines with the same LLM backbones. In particular, the performance increase using CoRoI on VQA^T is considerably significant, demonstrating its ability to handle distinct details from images by incorporating regions of interest from high-resolution images.

4.2.2 Component Analysis

Model Design We will begin by examining the design choices of the proposed method and presenting the results in Table 3. It is evident that the model demonstrates substantial improvements when our method is employed to enhance the original LLM baseline. For example, with LR and HR set to 336 and 672 respectively, the model achieves increase in the TextVQA and MME datasets. The addition of layers and positioning the attentive layers around the middle of the LLM further amplifies the performance, resulting in improvement in TextVQA compared to a single layer. These findings highlight the significant impact of our method in leveraging more

detailed visual cues. Furthermore, expanding the RoI numbers from 1 to 4 continues to yield additional improvements with our method. For instance, with 4 RoIs, it outperforms the baseline on the TextVQA [54], MME [20], and MM-Vet [63] datasets, respectively. The utilization of multi-scale high resolution images proves to be more advantageous than single-scale high resolution images. Using $2/3/4\times$ high resolution visual features are notably superior to the $2\times$ or $3\times$ counterparts, demonstrating the effectiveness of the designed modules with scaled-up input resolutions.

Dataset The importance of high-quality data cannot be emphasized enough for MLLMs. Our thorough analysis of the combined effects of different types of data, as shown in Table 4, starts with a base model that incorporates our method trained on the LLaVA-665K [35] instruction tuning data. By integrating high-quality captions from ShareGPT-4V [13], we observed improved visual alignment

and performance gains. We tested the model’s zero-shot performance on the TextVQA [54] benchmark, specifically by removing TextCaps [53] data from the training set as previous studies have done. This adjustment resulted in a significant decrease in performance, highlighting the importance of specific types of data in the training process. To address this decline, we introduced additional high-quality captions from LAION-GPT-4V [4] and OCR-specific data such as DocVQA [46] and AI2D [29] *etc.*, similar to the approach taken by [35], thereby enhancing the model’s OCR reasoning capabilities. By leveraging high-quality GPT-4V-generated responses from the ALLaVA [11] dataset, our framework was able to improve the baseline respectively on TextVQA and MMBench datasets. This comprehensive evaluation emphasizes the crucial role of strategic integration of high-quality data in maximizing the potential of our framework.

Table 4: Ablation on instruction-finetuning dataset, LLM input tokens: evaluated on VQA^T(TextVQA), MMBench and SEED benchmarks.

Method	Res.	LLM Tokens	VQA ^T	MMBench	SEED
LLaVA-1.5	336 ²	576	58.2	68.0	58.6
CoRoI-v1	336 ²	576	63.3	69.0	60.1
+ ShareGPT4V	336 ²	576	64.6	68.7	60.8
– TextCaps	336 ²	576	59.3	68.4	60.4
+ LAION-GPT4V	336 ²	576	61.2	68.4	61.0
+ DocVQA, AI2D, ChartQA, DVQA	336 ²	576	60.8	68.8	61.8
+ ALLaVA	336 ²	576	63.2	69.2	62.6
+ 2x Res. Token	336 ² +672 ²	2880	69.2	69.5	63.0

4.3 Model Qualitative Analysis

Visualization of the Selected Chain of Region-of-Interest As seen in Figure 3, CoRoI provides concise and correct answers in these two examples, whereas GPT-4V struggles to understand the visual spatial relationships or tends to produce hallucinated answers. On the right-hand side, we show the selected chain of regions of interest during model inference. It is evident that these regions can move reasonably over the high-resolution images and typically focus on the most informative areas. For example, in the code snippet example, the regions are centered around the ReLU and BatchNorm layers; in the Titanic example, the focused regions are crucial for answering the text questions accurately. This justifies the efficacy of integrating language clues in the RoI selection process.

5 Limitations

The highest resolution adopted in CoRoI is 1344×1344 , which may limit our model’s capability. However, this limitation primarily stems from a shortage of computational resources. Additionally, we employ interpolation methods for upsampling to obtain high-resolution images, but this process may result in the loss of some key information. Nevertheless, this issue mainly arises due to the lack of publicly available large-scale and high-quality high-resolution training data.

6 Conclusion

In this work, we introduce CoRoI, a visual instruction fine-tuning method utilizing the proposed Chain of Region-of-Interest approach. CoRoI aims to identify and prioritize the most informative regions in high-resolution images, thereby enhancing multimodal visual comprehension and recognition. We developed three model variants using CoRoI, ranging from 7B to 34B parameters. Extensive experiments on 11 benchmarks validate the efficacy of CoRoI across varying model sizes. We compared our models with both open-source models, such as LLaVA-NeXT, and closed-source models, such as Gemini Pro 1.0 and GPT-4V, demonstrating the superiority of our approach. Additionally,

we conducted extensive model analyses to understand the inner mechanisms and demonstrate its capability in solving real-world multimodal tasks.

References

- [1] Gpt-4v(ision) system card. https://cdn.openai.com/papers/GPTV_System_Card.pdf, 2023. 1, 2, 6, 7
- [2] Sharegpt. <https://sharegpt.com>, 2023. 7
- [3] The claude 3 model family: Opus, sonnet, haiku. https://www-cdn.anthropic.com/de8ba9b01c9ab7cbabf5c33b80b7bbc618857627/Model_Card_Claude_3.pdf, 2024. 2
- [4] Laion-gpt-4v dataset. <https://huggingface.co/datasets/laion/gpt4v-dataset>, 2024. 7, 8
- [5] Nous-hermes-2-yi-34b. <https://huggingface.co/NousResearch/Nous-Hermes-2-Yi-34B>, 2024. 6
- [6] Jean-Baptiste Alayrac, Jeff Donahue, Pauline Luc, Antoine Miech, Iain Barr, Yana Hasson, Karel Lenc, Arthur Mensch, Katherine Millican, Malcolm Reynolds, et al. Flamingo: a visual language model for few-shot learning. *NeurIPS*, 2022. 1, 2, 3
- [7] Stanislaw Antol, Aishwarya Agrawal, Jiasen Lu, Margaret Mitchell, Dhruv Batra, C. Lawrence Zitnick, and Devi Parikh. VQA: Visual Question Answering. In *ICCV*, 2015. 2, 7
- [8] Anas Awadalla, Irena Gao, Joshua Gardner, Jack Hessel, Yusuf Hanafy, Wanrong Zhu, Kalyani Marathe, Yonatan Bitton, Samir Gadre, Jenia Jitsev, Simon Kornblith, Pang Wei Koh, Gabriel Ilharco, Mitchell Wortsman, and Ludwig Schmidt. Openflamingo, Mar. 2023. 2
- [9] Jinze Bai, Shuai Bai, Shusheng Yang, Shijie Wang, Sinan Tan, Peng Wang, Junyang Lin, Chang Zhou, and Jingren Zhou. Qwen-vl: A versatile vision-language model for understanding, localization, text reading, and beyond. *arXiv preprint arXiv:2308.12966*, 2023. 6, 7
- [10] Tom Brown, Benjamin Mann, Nick Ryder, Melanie Subbiah, Jared D Kaplan, Prafulla Dhariwal, Arvind Neelakantan, Pranav Shyam, Girish Sastry, Amanda Askell, et al. Language models are few-shot learners. *NeurIPS*, 2020. 2
- [11] Guiming Hardy Chen, Shunian Chen, Ruifei Zhang, Junying Chen, Xiangbo Wu, Zhiyi Zhang, Zhihong Chen, Jianquan Li, Xiang Wan, and Benyou Wang. Allava: Harnessing gpt4v-synthesized data for a lite vision-language model. *arXiv preprint arXiv:2402.11684*, 2024. 6, 7, 8
- [12] Keqin Chen, Zhao Zhang, Weili Zeng, Richong Zhang, Feng Zhu, and Rui Zhao. Shikra: Unleashing multimodal llm’s referential dialogue magic. *arXiv preprint arXiv:2306.15195*, 2023. 6
- [13] Lin Chen, Jisong Li, Xiaoyi Dong, Pan Zhang, Conghui He, Jiaqi Wang, Feng Zhao, and Dahua Lin. Sharegpt4v: Improving large multi-modal models with better captions. *arXiv preprint arXiv:2311.12793*, 2023. 7, 8
- [14] Yixin Chen, Shuai Zhang, Boran Han, Tong He, and Bo Li. Camml: Context-aware multimodal learner for large models. *arXiv preprint arXiv:2401.03149*, 2024. 3
- [15] Zhe Chen, Weiyun Wang, Hao Tian, Shenglong Ye, Zhangwei Gao, Erfei Cui, Wenwen Tong, Kongzhi Hu, Jiapeng Luo, Zheng Ma, Ji Ma, Jiaqi Wang, Xiaoyi Dong, Hang Yan, Hewei Guo, Conghui He, Botian Shi, Zhenjiang Jin, Chao Xu, Bin Wang, Xingjian Wei, Wei Li, Wenjian Zhang, Bo Zhang, Pinlong Cai, Licheng Wen, Xiangchao Yan, Min Dou, Lewei Lu, Xizhou Zhu, Tong Lu, Dahua Lin, Yu Qiao, Jifeng Dai, and Wenhai Wang. How far are we to gpt-4v? closing the gap to commercial multimodal models with open-source suites, 2024. 1, 3
- [16] Xiangxiang Chu, Limeng Qiao, Xinyu Zhang, Shuang Xu, Fei Wei, Yang Yang, Xiaofei Sun, Yiming Hu, Xinyang Lin, Bo Zhang, et al. Mobilevlm v2: Faster and stronger baseline for vision language model. *arXiv preprint arXiv:2402.03766*, 2024. 6
- [17] Wenliang Dai, Junnan Li, Dongxu Li, Anthony Meng Huat Tiong, Junqi Zhao, Weisheng Wang, Boyang Li, Pascale Fung, and Steven Hoi. Instructblip: Towards general-purpose vision-language models with instruction tuning, 2023. 6
- [18] Xiaoyi Dong, Pan Zhang, Yuhang Zang, Yuhang Cao, Bin Wang, Linke Ouyang, Songyang Zhang, Haodong Duan, Wenwei Zhang, Yining Li, Hang Yan, Yang Gao, Zhe Chen, Xinyue Zhang, Wei Li, Jingwen Li, Wenhai Wang, Kai Chen, Conghui He, Xingcheng Zhang, Jifeng Dai, Yu Qiao, Dahua Lin, and Jiaqi Wang. Internlm-xcomposer2-4khd: A pioneering large vision-language model handling resolutions from 336 pixels to 4k hd, 2024. 1, 3
- [19] Alexey Dosovitskiy, Lucas Beyer, Alexander Kolesnikov, Dirk Weissenborn, Xiaohua Zhai, Thomas Unterthiner, Mostafa Dehghani, Matthias Minderer, Georg Heigold, Sylvain Gelly, Jakob Uszkoreit, and Neil Houlsby. An image is worth 16x16 words: Transformers for image recognition at scale. *ICLR*, 2021. 2
- [20] Chaoyou Fu, Peixian Chen, Yunhang Shen, Yulei Qin, Mengdan Zhang, Xu Lin, Zhenyu Qiu, Wei Lin, Jinrui Yang, Xiawu Zheng, Ke Li, Xing Sun, and Rongrong Ji. Mme: A comprehensive evaluation benchmark for multimodal large language models. *arXiv preprint arXiv:2306.13394*, 2023. 2, 7, 8
- [21] Danna Gurari, Qing Li, Abigale J Stangl, Anhong Guo, Chi Lin, Kristen Grauman, Jiebo Luo, and Jeffrey P Bigham. Vizwiz grand challenge: Answering visual questions from blind people. *CVPR*, 2018. 2, 7
- [22] Wenyi Hong, Weihang Wang, Qingsong Lv, Jiazheng Xu, Wenmeng Yu, Junhui Ji, Yan Wang, Zihan Wang, Yuxiao Dong, Ming Ding, et al. Cogagent: A visual language model for gui agents. *arXiv preprint arXiv:2312.08914*, 2023. 1, 2, 3
- [23] Drew A. Hudson and Christopher D. Manning. GQA: A new dataset for real-world visual reasoning and compositional question answering. In *CVPR*, 2019. 2, 7
- [24] Andrew Jaegle, Sebastian Borgeaud, Jean-Baptiste Alayrac, Carl Doersch, Catalin Ionescu, David Ding, Skanda Koppula, Daniel Zoran, Andrew Brock, Evan Shelhamer, Olivier J. Hénaff, Matthew M. Botvinick,

- Andrew Zisserman, Oriol Vinyals, and João Carreira. Perceiver IO: A general architecture for structured inputs & outputs. In *ICLR*, 2022. 3
- [25] Andrew Jaegle, Felix Gimeno, Andy Brock, Oriol Vinyals, Andrew Zisserman, and João Carreira. Perceiver: General perception with iterative attention. In *ICML*, 2021. 3
- [26] Albert Q. Jiang, Alexandre Sablayrolles, Arthur Mensch, Chris Bamford, Devendra Singh Chaplot, Diego de las Casas, Florian Bressand, Gianna Lengyel, Guillaume Lample, Lucile Saulnier, L  lio Renard Lavaud, Marie-Anne Lachaux, Pierre Stock, Teven Le Scao, Thibaut Lavril, Thomas Wang, Timoth  e Lacroix, and William El Sayed. Mistral 7b, 2023. 6
- [27] Albert Q. Jiang, Alexandre Sablayrolles, Antoine Roux, Arthur Mensch, Blanche Savary, Chris Bamford, Devendra Singh Chaplot, Diego de las Casas, Emma Bou Hanna, Florian Bressand, Gianna Lengyel, Guillaume Bour, Guillaume Lample, L  lio Renard Lavaud, Lucile Saulnier, Marie-Anne Lachaux, Pierre Stock, Sandeep Subramanian, Sophia Yang, Szymon Antoniak, Teven Le Scao, Th  ophile Gervet, Thibaut Lavril, Thomas Wang, Timoth  e Lacroix, and William El Sayed. Mixtral of experts, 2024. 2
- [28] Kushal Kaffle, Scott Cohen, Brian Price, and Christopher Kanan. Dvqa: Understanding data visualizations via question answering. In *CVPR*, 2018. 7
- [29] Aniruddha Kembhavi, Michael Salvato, Eric Kolve, Minjoon Seo, Hannaneh Hajishirzi, and Ali Farhadi. A diagram is worth a dozen images. *ArXiv*, abs/1603.07396, 2016. 7, 8
- [30] Ranjay Krishna, Yuke Zhu, Oliver Groth, Justin Johnson, Kenji Hata, Joshua Kravitz, Stephanie Chen, Yannis Kalantidis, Li-Jia Li, David A. Shamma, Michael S. Bernstein, and Li Fei-Fei. Visual genome: Connecting language and vision using crowdsourced dense image annotations. *International Journal of Computer Vision*, 2017. 7
- [31] Hugo Lauren  on, Lucile Saulnier, L  o Tronchon, Stas Bekman, Amanpreet Singh, Anton Lozhkov, Thomas Wang, Siddharth Karamcheti, Alexander M. Rush, Douwe Kiela, Matthieu Cord, and Victor Sanh. Obelics: An open web-scale filtered dataset of interleaved image-text documents, 2023. 6
- [32] Bohao Li, Rui Wang, Guangzhi Wang, Yuying Ge, Yixiao Ge, and Ying Shan. Seed-bench: Benchmarking multimodal llms with generative comprehension, 2023. 2, 7
- [33] Bo Li, Peiyuan Zhang, Jingkan Yang, Yuanhan Zhang, Fanyi Pu, and Ziwei Liu. Otterhd: A high-resolution multi-modality model. *arXiv preprint arXiv:2311.04219*, 2023. 1, 3, 6
- [34] Junnan Li, Dongxu Li, Silvio Savarese, and Steven C. H. Hoi. BLIP-2: bootstrapping language-image pre-training with frozen image encoders and large language models. *CoRR*, 2023. 2
- [35] Haotian Liu, Chunyuan Li, Yuheng Li, and Yong Jae Lee. Improved baselines with visual instruction tuning. *arXiv preprint arXiv:2310.03744*, 2023. 1, 2, 3, 6, 8
- [36] Haotian Liu, Chunyuan Li, Yuheng Li, Bo Li, Yuanhan Zhang, Sheng Shen, and Yong Jae Lee. Llava-next: Improved reasoning, ocr, and world knowledge, 2024. 1, 2, 3, 6
- [37] Haotian Liu, Chunyuan Li, Qingyang Wu, and Yong Jae Lee. Visual instruction tuning. *Thirty-seventh Conference on Neural Information Processing Systems*, 2023. 1, 2, 3, 5, 7
- [38] Yuan Liu, Haodong Duan, Yuanhan Zhang, Bo Li, Songyang Zhnag, Wangbo Zhao, Yike Yuan, Jiaqi Wang, Conghui He, Ziwei Liu, Kai Chen, and Dahua Lin. Mmbench: Is your multi-modal model an all-around player? *arXiv:2307.06281*, 2023. 2, 7
- [39] Jiasen Lu, Christopher Clark, Rowan Zellers, Roozbeh Mottaghi, and Aniruddha Kembhavi. UNIFIED-IO: A unified model for vision, language, and multi-modal tasks. In *The Eleventh International Conference on Learning Representations*, 2023. 3
- [40] Pan Lu, Hritik Bansal, Tony Xia, Jiacheng Liu, Chunyuan Li, Hannaneh Hajishirzi, Hao Cheng, Kai-Wei Chang, Michel Galley, and Jianfeng Gao. Mathvista: Evaluating mathematical reasoning of foundation models in visual contexts. In *International Conference on Learning Representations (ICLR)*, 2024. 2, 7
- [41] Pan Lu, Swaroop Mishra, Tony Xia, Liang Qiu, Kai-Wei Chang, Song-Chun Zhu, Oyvind Tafjord, Peter Clark, and Ashwin Kalyan. Learn to explain: Multimodal reasoning via thought chains for science question answering. In *The 36th Conference on Neural Information Processing Systems (NeurIPS)*, 2022. 2, 7
- [42] Gen Luo, Yiyi Zhou, Jiamu Sun, Xiaoshuai Sun, and Rongrong Ji. A survivor in the era of large-scale pretraining: An empirical study of one-stage referring expression comprehension. *IEEE Transactions on Multimedia*, 26:3689–3700, 2024. 1, 3
- [43] Gen Luo, Yiyi Zhou, Yuxin Zhang, Xiawu Zheng, Xiaoshuai Sun, and Rongrong Ji. Feast your eyes: Mixture-of-resolution adaptation for multimodal large language models, 2024. 1, 3, 6
- [44] Kenneth Marino, Mohammad Rastegari, Ali Farhadi, and Roozbeh Mottaghi. Ok-vqa: A visual question answering benchmark requiring external knowledge. In *CVPR*, 2019. 7
- [45] Ahmed Masry, Do Long, Jia Qing Tan, Shafiq Joty, and Enamul Hoque. ChartQA: A benchmark for question answering about charts with visual and logical reasoning. In *Findings of the Association for Computational Linguistics: ACL 2022*, 2022. 7
- [46] Minesh Mathew, Dimosthenis Karatzas, and C. V. Jawahar. Docvqa: A dataset for vqa on document images, 2021. 7, 8
- [47] Anand Mishra, Shashank Shekhar, Ajeet Kumar Singh, and Anirban Chakraborty. Ocr-vqa: Visual question answering by reading text in images. In *ICDAR*, 2019. 7
- [48] OpenAI. Gpt-4 technical report, 2023. 2
- [49] Alec Radford, Jong Wook Kim, Chris Hallacy, Aditya Ramesh, Gabriel Goh, Sandhini Agarwal, Girish Sastry, Amanda Askell, Pamela Mishkin, Jack Clark, et al. Learning transferable visual models from natural language supervision. In *ICML*. PMLR, 2021. 2, 5

- [50] Jeff Rasley, Samyam Rajbhandari, Olatunji Ruwase, and Yuxiong He. Deepspeed: System optimizations enable training deep learning models with over 100 billion parameters. In *Proceedings of the 26th ACM SIGKDD International Conference on Knowledge Discovery & Data Mining*, pages 3505–3506, 2020. 6
- [51] Dustin Schwenk, Apoorv Khandelwal, Christopher Clark, Kenneth Marino, and Roozbeh Mottaghi. A-okvqa: A benchmark for visual question answering using world knowledge. *arXiv*, 2022. 7
- [52] Mustafa Shukor, Corentin Dancette, Alexandre Rame, and Matthieu Cord. Unified model for image, video, audio and language tasks, 2023. 3
- [53] Oleksii Sidorov, Ronghang Hu, Marcus Rohrbach, and Amanpreet Singh. Textcaps: a dataset for image captioning with reading comprehension. 2020. 7, 8
- [54] Amanpreet Singh, Vivek Natarjan, Meet Shah, Yu Jiang, Xinlei Chen, Devi Parikh, and Marcus Rohrbach. Towards vqa models that can read. In *CVPR*, 2019. 2, 8
- [55] Chameleon Team. Chameleon: Mixed-modal early-fusion foundation models. *arXiv e-prints*, pages arXiv–2405, 2024. 3
- [56] Gemini Team, Rohan Anil, Sebastian Borgeaud, Yonghui Wu, Jean-Baptiste Alayrac, Jiahui Yu, Radu Soricut, Johan Schalkwyk, Andrew M Dai, Anja Hauth, et al. Gemini: a family of highly capable multimodal models. *arXiv preprint arXiv:2312.11805*, 2023. 1, 2, 6, 7
- [57] Shengbang Tong, Zhuang Liu, Yuexiang Zhai, Yi Ma, Yann LeCun, and Saining Xie. Eyes wide shut? exploring the visual shortcomings of multimodal llms. *arXiv preprint arXiv:2401.06209*, 2024. 1, 3
- [58] Hugo Touvron, Thibaut Lavril, Gautier Izacard, Xavier Martinet, Marie-Anne Lachaux, Timothée Lacroix, Baptiste Rozière, Naman Goyal, Eric Hambro, Faisal Azhar, Aurelien Rodriguez, Armand Joulin, Edouard Grave, and Guillaume Lample. Llama: Open and efficient foundation language models, 2023. 2
- [59] Maria Tsimpoukelli, Jacob Menick, Serkan Cabi, S. M. Ali Eslami, Oriol Vinyals, and Felix Hill. Multi-modal few-shot learning with frozen language models. In *NeurIPS*, 2021. 1, 3
- [60] Peng Wang, An Yang, Rui Men, Junyang Lin, Shuai Bai, Zhikang Li, Jianxin Ma, Chang Zhou, Jingren Zhou, and Hongxia Yang. Ofa: Unifying architectures, tasks, and modalities through a simple sequence-to-sequence learning framework. In *ICML*. PMLR, 2022. 1, 3
- [61] Weihang Wang, Qingsong Lv, Wenmeng Yu, Wenyi Hong, Ji Qi, Yan Wang, Junhui Ji, Zhuoyi Yang, Lei Zhao, Xixuan Song, et al. Cogvlm: Visual expert for pretrained language models. *arXiv preprint arXiv:2311.03079*, 2023. 1, 2, 3, 6
- [62] Licheng Yu, Patrick Poirson, Shan Yang, Alexander C. Berg, and Tamara L. Berg. Modeling context in referring expressions. In Bastian Leibe, Jiri Matas, Nicu Sebe, and Max Welling, editors, *ECCV*, 2016. 7
- [63] Weihao Yu, Zhengyuan Yang, Linjie Li, Jianfeng Wang, Kevin Lin, Zicheng Liu, Xinchao Wang, and Lijuan Wang. Mm-vet: Evaluating large multimodal models for integrated capabilities, 2023. 2, 7, 8
- [64] Xiang Yue, Yuansheng Ni, Kai Zhang, Tianyu Zheng, Ruoqi Liu, Ge Zhang, Samuel Stevens, Dongfu Jiang, Weiming Ren, Yuxuan Sun, Cong Wei, Botao Yu, Ruibin Yuan, Renliang Sun, Ming Yin, Boyuan Zheng, Zhenzhu Yang, Yibo Liu, Wenhao Huang, Huan Sun, Yu Su, and Wenhua Chen. Mmmu: A massive multi-discipline multimodal understanding and reasoning benchmark for expert agi. In *Proceedings of CVPR*, 2024. 2, 7
- [65] Renrui Zhang, Jiaming Han, Aojun Zhou, Xiangfei Hu, Shilin Yan, Pan Lu, Hongsheng Li, Peng Gao, and Yu Qiao. Llama-adapter: Efficient fine-tuning of language models with zero-init attention. *arXiv preprint arXiv:2303.16199*, 2023. 1, 2, 3
- [66] Deyao Zhu, Jun Chen, Xiaoqian Shen, Xiang Li, and Mohamed Elhoseiny. Minigpt-4: Enhancing vision-language understanding with advanced large language models. *arXiv preprint arXiv:2304.10592*, 2023. 1, 3
- [67] Xizhou Zhu, Jinguo Zhu, Hao Li, Xiaoshi Wu, Hongsheng Li, Xiaohua Wang, and Jifeng Dai. Uni-perceiver: Pre-training unified architecture for generic perception for zero-shot and few-shot tasks. In *CVPR*, 2022. 3

A Appendix

Experimental Details We present the experimental details of our model here. The default layers location k is determined by first uniformly dividing all LLM layers into 4 sections, then doubling the layers within the section close to the middle of LLM. For example, using 32 layers Mistral-7B, we initially select $\{7, 15, 23\}$ layers and then double the layers to $\{7, 11, 15, 19, 23, 27\}$. This process is same for other LLMs with different layers. The default RoI number n is set to 4, and the multi-scale HR Resolution m, λ is set to 3 and $2/3/4\times$, respectively.

Reasoning Generative Ability In Figure 5, We also demonstrate CoRoI’s ability in generative reasoning, which means that when given an image, CoRoI can firstly reason from it then produce text with image-generation prompts based on instructions. In Sponge-Bob example, CoRoI is capable of generating a story accompanied by multiple illustrative images. Also, in the Golden Gate Bridge scenario, CoRoI can edit the source image in various ways. In the pizza example, CoRoI can analyze the image and given ingredients to produce an article and illustrative image for making the pizza.

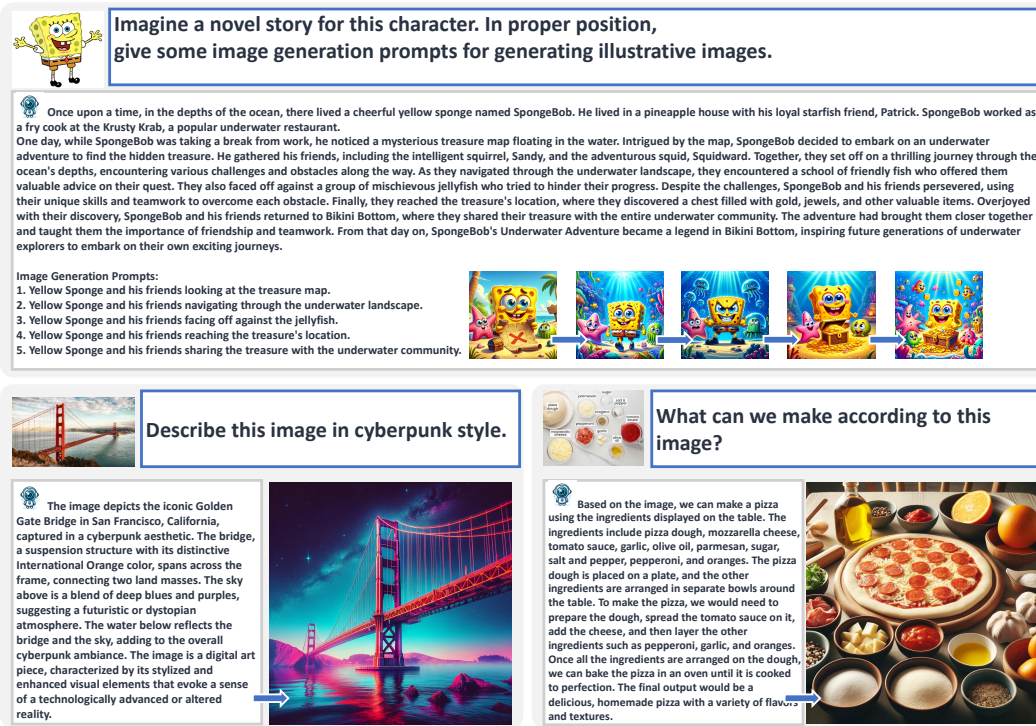


Figure 5: Reasoning Generative Capability. The generated images are from DALL-E3 using prompts generated by CoRoI.